

Optimal Control of a Subway System with Wayside Energy Storage using Deterministic Dynamic Programming

Erick Froede
Chris Melville
Mike Rothenberger

December 16, 2011

Abstract

The purpose of this paper is to apply a deterministic dynamic programming (DDP) solution to a metro transit system consisting of two stations, external power grid, flywheel wayside energy storage unit, and a single subway train. Previous approaches have been predominantly application based and qualitative, rather than quantitative, in their analysis. Our solution successfully creates an optimal trajectory which is cyclic in nature, allowing the train to pass between stations while maintaining a minimum energy in the flywheel wayside energy storage system (WESS). Additionally, the case without energy storage was briefly examined, and the result indicates there is significant energy savings potential for a system with regenerative energy storage.

1 Introduction

This paper develops an optimal subway train acceleration and deceleration profile with respect to the energy usage of an external power source and wayside energy storage system (WESS). Given fixed distance, time, and operational constraints the system's performance will be maintained for every cycle. Our analysis will take advantage of the regenerative braking capability of traction motors to allow the train to both draw and supply power. Based on the costs of each action with regard to power prices as well as resistive losses in the third rail, an optimal path will be produced via deterministic dynamic programming (DDP), a tool that can be used to compute the optimal trajectory of a constrained problem. DDP is a backward stepping algorithm that examines the current cost, the transition cost of a particular move, and which sum of the two costs will be the least. In this manner, the overarching solution is composed of smaller optimal sub trajectories. It is critical to develop a cost function and transition matrix which accurately represent the problem while also being manageable in complexity. To begin this process, we examined the available literature concerning subway energy storage systems.

1.1 Energy Saving Potential

Currently, subway cars are powered by a third rail, usually running between or next to the tracks on which the wheels reside. It carries DC current up to 1500 V, and is an alternative to the traditional overhead wire systems used in above ground train systems. During acceleration away from the station power is drawn from this third rail to drive electric traction motors, and during deceleration the generated current is dissipated as heat through under floor resistor grids [1]. Applying energy saving devices to improve this model is not a new concept, and is driven by the continued demand for mass transit services at lower energy cost and environmental impact. The planet now has 182 metro systems, transporting 102 million passengers daily over a combined 10,542 km of track, so the potential exists that small efficiency gains will have a wide ranging impact [2]. A number of ideas have been developed to address this concern over the years, with super capacitors and flywheel energy storage being the prime candidates; both of these technologies are able to take advantage of the frequent charge and discharge cycles characteristic of subway transit [3].

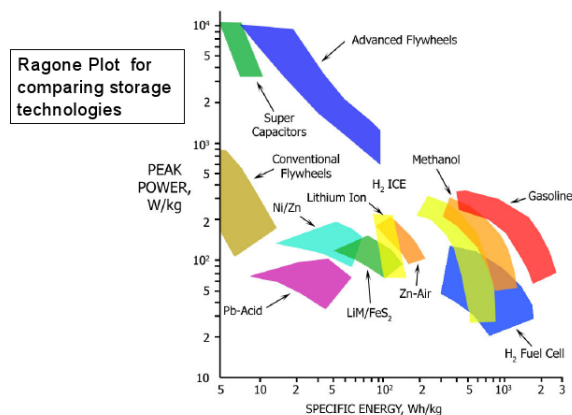


Figure 1: Peak power versus specific energy for various energy storage technologies [4].

However, as illustrated by Figure 1, advanced composite flywheels provide significant advantages in specific energy while providing equivalent peak power when compared to super capacitors.

1.2 Flywheel Technology

When examining flywheels there are a number of technical characteristics that are particularly important. First, losses can play a significant factor, namely through bearing friction and windage. In order to address this, modern systems incorporate magnetic bearings and vacuum environments, which help alleviate these issues to a large degree. Additionally, flywheels were once typically made of dense metal and limited in maximum rotational velocity due to the risk of a material flaw and the ensuing safety concerns. In response, composite flywheels have been developed which are both more structurally sound and safer if failure occurs [5]. A summary of key flywheel facts can be seen below in Table 1, with energy values specifically pertaining to train-capable systems.

Table 1: Selected Flywheel Characteristics [5]

Category	Value
Storage Mechanism	Mechanical
Rotor Material	Metal or Composite
Rotor Mass (kg)	2500
Service Lifetime (years)	>20
Number of Manufacturers	Approx. 10
Peak Power (kW)	2
Stored Energy (MJ)	470
Rotational Velocity (rpm)	15,000
Rim Speed (m/s)	950
Charge Storage Time	Hours
Price per kW (\$)	400-800

1.3 Optimal Control of Flywheels

When implementing flywheels, there are two potential options: onboard storage or a WESS. A 1971 study sponsored by the Urban Mass Transportation Administration (UMTA) under the Department of Transportation (DOT) represented the “world’s first use of the energy storing flywheel to propel subway transit cars”. The New York Metro Transit Authority (MTA) reported an energy savings of 25-40% on complete route runs, depending on the type of service [6, 7].

Another major work addressing onboard flywheel energy storage during this time period was “Regenerative Drive for Subway Trains” by Flanagan and Suokas. Much like the previous study, a real life mass transit system was examined, namely the Toronto Bloor-Danforth subway line. However, these two landmark investigations differ because this particular case utilized numerical optimization

of the flywheel control system, representing a significant theoretical advance and the first instance where control theory was applied. Their control system implemented a finite difference method in which two numerical models were created: one governing the equations of motion for the flywheel and another for the track itself. In creating these equations of motion the flywheel shape, size, material, losses, and operational ranges were considered in detail, representing the most in-depth mechanical analysis with respect to subway integration performed up to that point. As for the track model, due to real data provided by the Toronto Transit Commission (TTC) several key aspects could be considered, such as track grades, curvature, and accurate station distances. Additionally, acceleration and deceleration profiles which operators used in common practice were defined, adding further realism as passenger comfort was implicitly considered for the first time (an idea which was extended to energy conservation as well [8]). As a result of their efforts, the authors concluded that flywheel energy storage would result in 26 percent energy savings for the Bloor-Danforth subway line on a daily round trip basis, even considering various vehicle load ranges [9, 10, 11, 12].

1.4 Feasibility for Energy Storage

One particular paper that directly resulted from the early feasibility studies was “Wayside Energy Storage for Recuperation of Potential Energy from Freight Trains” by Lawson et al., initiated by the DOT’s research activities in 1977. The purpose was “to determine whether or not wayside energy storage, using present state-of-the-art technology, could provide a cost-effective means of reducing the high energy consumption of railroad freight operations on grades”. First, the authors attempted to determine if flywheel storage was indeed the best technology to use in a rail application with heavy loads and unique acceleration and braking characteristics. This was accomplished by a comparative technical study which considered batteries, compressed air, hydroelectric, and traditional utility supplies alongside flywheels. Ultimately, it was found that flywheels are indeed the most economic and efficient method for storing energy with consumption at a later time; in particular, it had strengths in round trip efficiency, cycle life, and service life. When an optimal flywheel design, which is outlined in the paper, was applied to the various lines being considered it was found that WESS has significant viability. For example, it was calculated that the Los Angeles - Belen route could potentially save 27.82 million gallons annually based on 1990 traffic levels [13].

At the end of this study, the authors state that “WESS is highly compatible with presently electrified railroads and can affect substantial economies by shaving the peak demand”. Furthermore, “the WESS concept enhances the economics of railroad electrification and permits evolutionary electrification of complete routes”, and “the flywheel technology required for WESS can be based on the state of

the art . . . future improvements in composite flywheel fabrication techniques should reduce costs and make larger capacity flywheels possible” [13, 14].

1.5 Contemporary Work on Flywheels

After the progress made in 1976 and 1977 by Flanagan et al. as well as the DOT, the literature regarding flywheel energy storage in mass transit largely went silent until 2009 when Barrero et al. published “Stationary or Onboard Energy Storage Systems for Energy Consumption Reduction in a Metro Network”. While examining capacitive energy storage rather than flywheels, this paper was important because it used a modern modeling and simulation method in combination with real data from a Brussels metro line to determine the viability of an energy storage system (ESS). The particular tool used in this case was a “quasi-static” backwards looking model, which integrated a network model with representations for the subway vehicle, ESS, and external power supply in terms of both electrical and mechanical state equations. One of the key aspects considered were track resistances, which represent the first effort to implement dynamics of this type [15]. A representation of this network model can be seen below, in Figure 2:

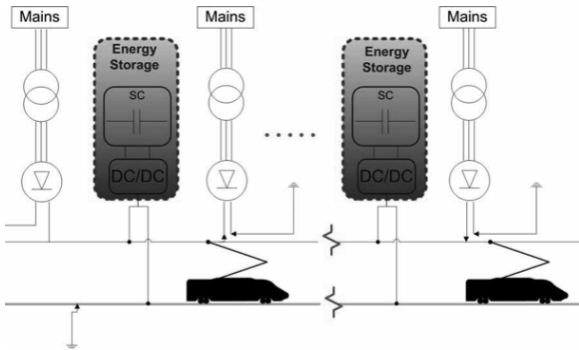


Figure 2: Network Model with Subway Vehicles, ESS, and External Power Supply [15].

When both options were considered, the authors concluded that if vehicle autonomy is not an issue and the electrical network can cope with relatively large power peaks, the stationary ESS is a more reasonable option; this is due to lower installed capacity requirements, ease of installation, elimination of retrofitting, and good simulation results [15].

Further contemporary support for the use of WESS flywheels in metro systems can be found in the paper “Stationary Applications of Energy Storage Technologies for Transit Systems” by Radcliffe et al., which details its application in the London underground’s Piccadilly line. If this optimal system was present, it was estimated that energy consumption could be reduced by up to 26% and investment payback would occur within five years [16].

2 Methodology

To explore how the regenerative braking energy of a subway train can be stored with a WESS we wanted to modeled a specific case where there were two stations and two flywheels as shown in Figure 3. In order to allow the simulation to arrive at an optimal solution in a reasonable time-frame the model was simplified to one flywheel between two stations.

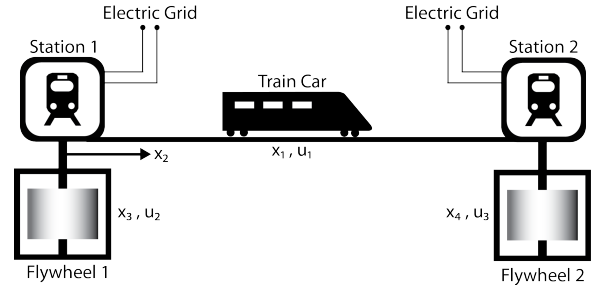


Figure 3: Specific case with two stations and two flywheels.

In section 2.1 we’ll consider the system dynamics governing the velocity and position of the train as well as the energy storage of the flywheel. In section 2.2 the static algebraic constraints which define the electrical system for each time instant will be examined.

2.1 Modeling Equations

Our states are the velocity of the train, the position of the train and the velocity of the flywheel. The velocity can be derived from the governing equation for the train:

$$m_1 \dot{v} = F_{input} - F_{rolling} - F_{aero} \quad (1)$$

Based on the notation shown in Figure 4:

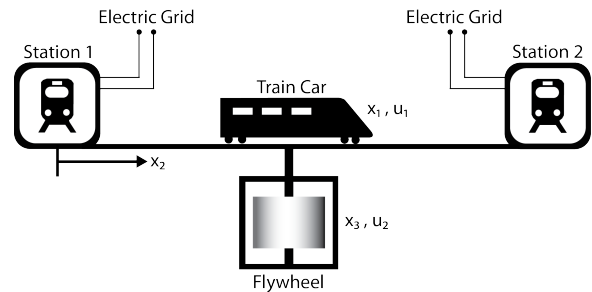


Figure 4: Simplified case with one flywheel between two stations.

$$m_1 \dot{x}_1 = u_1 - f_r m_1 g - \frac{1}{2} C_w A \rho x_1^2 \quad (2)$$

In this equation x_1 is the train velocity and u_1 is the input force on the train. The mass of the train is m_1 and

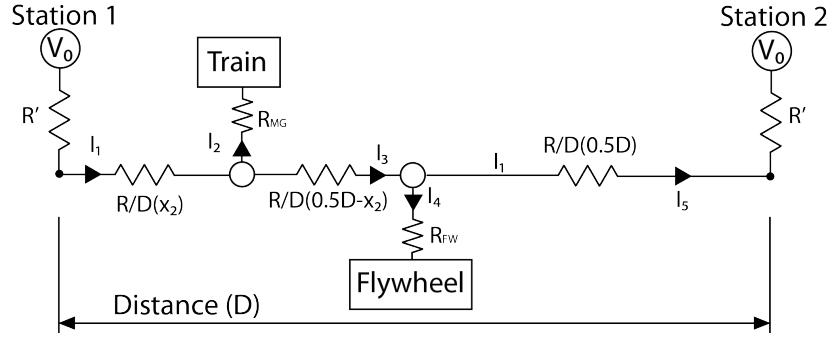


Figure 5: Electrical equivalent circuit for case 1 (train between station 1 and flywheel).

gravity is defined as g . Rolling resistance of a steel wheel on a steel rail is f_r , the aerodynamic drag coefficient is C_w , the frontal area of the train is A , and the air density is ρ . Velocity is the time derivative of position, so our second governing relation is:

$$\dot{x} = v \quad (3)$$

Changing the variables to match our state equation notation shown in Figure 4, where x_2 is the distance the train has travelled from station 1, we get:

$$\dot{x}_2 = x_1 \quad (4)$$

The governing equation of the flywheel is:

$$I\dot{\omega} = T_{input} - c\omega^2 \quad (5)$$

The term ω is the rotational velocity of the flywheel. Substituting for I , the moment of inertia, and changing to state equation notation where x_3 is the flywheel speed, this becomes:

$$\frac{1}{2}m_2r^2\dot{x}_3 = u_2 - cx_3^2 \quad (6)$$

The terms m_2 and r are the mass and radius of the flywheel respectively, u_2 is the input torque and c is a term accounting for losses over time.

2.2 Problem Constraints

This section enumerates a few values which are critical to the problem setup: the station-to-station distance, the top speed of the train, and the acceleration of the train and flywheel. We started by selecting a maximum desirable train acceleration of 1 m/s^2 and we estimated a reasonable train mass to be 50000 kg based on the available literature. Using the estimated train mass and the maximum allowed acceleration we determined the bounds of the force on the train to be $-50 - 50 \text{ kN}$. For the given track length of 1000 m , the six given time steps of 20 seconds, and the maximum allowed acceleration of 1 m/s^2 we were able to determine velocity bounds of $0 - 20 \text{ m/s}$. Based on a survey

of the literature we chose a normal operating velocity for the system's flywheel of 1310 rad/s and a flywheel mass of 2500 kg . We chose the flywheel torque range to be $-450 - 450 \text{ N-m}$ so that the flywheel would be able to supply or absorb the majority of the power to or from the train. Then from Newton's Second Law the range of flywheel speeds was determined to be $1290 - 1330 \text{ rad/s}$. The estimated resistances to represent the motor and flywheel efficiencies were set at 0.185Ω to give a reasonable range of values.

2.3 Static Equations

In order to understand the interactions between electrical current and voltage Figure 4 was converted to an electrical representation, shown in Figure 5. Equations 7 and 8 were derived using Kirchhoff's current law with Figure 5 as a guide. Starting with a node analysis at the two nodes in the system, Kirchhoff's current law yields:

$$I_1 = I_2 + I_3 \quad (7)$$

$$I_3 = I_4 + I_5 \quad (8)$$

In equations 7 and 8, I_1 and I_5 are electrical currents to or from the external power source. The electrical currents I_2 and I_4 in these equations are the electrical currents to the train and flywheel respectively. Finally, I_3 is the third-rail current between the train and the flywheel. The nominal electrical current directions are shown in Figure 5.

Next we develop the equations for power to the train and flywheel, in that order:

$$u_1x_1 = I_2(V_0 - I_1(R' + \frac{R}{D}x_2) - I_2R_{MG}) \quad (9)$$

$$u_2x_3 = I_4(V_0 - I_1(R' + \frac{R}{D}x_2) - I_3\frac{R}{D}(0.5D - x_2) - I_4R_{FW}) \quad (10)$$

We are equating the mechanical power of the train and flywheel to the DC electrical power supplied through

the third rail. Here, R' is an effective substation resistance, R/D is a per-meter third rail resistance, and R_{MG} and R_{FW} are effective resistances that represent efficiency losses in the traction and flywheel motors respectively. Finally, by Kirchhoff's voltage law we arrive at:

$$I_5(R' + \frac{R}{D}(0.5D)) = -I_1(R' + \frac{R}{D}x_2) - I_3\frac{R}{D}(0.5D - x_2) \quad (11)$$

This equation shows the voltage drop from station 1 power supply to the flywheel node must be the same as the voltage drop from station 2 to the flywheel node.

In the case shown the train is between station one and the flywheel; there is another separate but similar set of equations for the case where the train is between the flywheel and station 2. For this separate derivation refer to appendix A.

The solution to these equations is generated numerically using the MATLAB function FSOLVE. This function uses one of three algorithms, defaulting to the trust-region-dogleg algorithm. We were not able to solve the system of equations for every combination of states and inputs but the ones that did not converge to the correct solution appear to be in the infeasible region.

After the system of equations is solved for every state and input, the net power into and out of the system from the power supply is calculated. Given the ratio of purchase to resale cost being 3.33, the total cost of each combination of states and inputs is generated and stored in a five dimensional table, indexed to the corresponding states and inputs. This is our transition cost table, which will be called in our deterministic dynamic programming (DDP) code to minimize power into and out of the power supply.

2.4 Dynamic Programming

For our analysis we will use Bellman's optimality principle to find the optimal sub-paths and thus the optimal path. According to Bellman's principle, for a path to be optimal every conceivable sub-path must also be the optimal trajectory between the two points. For an in depth discussion of Bellman's optimality principle which is beyond the scope of this discussion, refer to Bertsekas [17].

There are two main reasons why we are considering this problem as deterministic. The first is that we know the states and inputs at the terminal state (station two). A stochastic model where the flywheel terminal state is unknown could also be valid, but we have simplified this problem by constraining the flywheel terminal velocity. The primary feature of the system which allows us to make this assumption is that the trains will be accelerating and braking in the same areas. In order to minimize grid energy consumption regenerated braking energy must be stored. Without the flywheel end state constraint the energy stored

in the flywheel would continually decrease with each passing train and the system would no longer be deterministic.

We proceed by stepping backwards from the terminal point and comparing the cost of transition from the current time step to the next time step forward for every possible state and input combination as represented by the valley in Figure 6. By selecting the minimum transition cost and saving it to an additive cost to go matrix we ensure that every step backwards is optimal. This allows us to construct the overall optimal path by recording the states and inputs that generate the lowest cost route as shown in Figure 7.

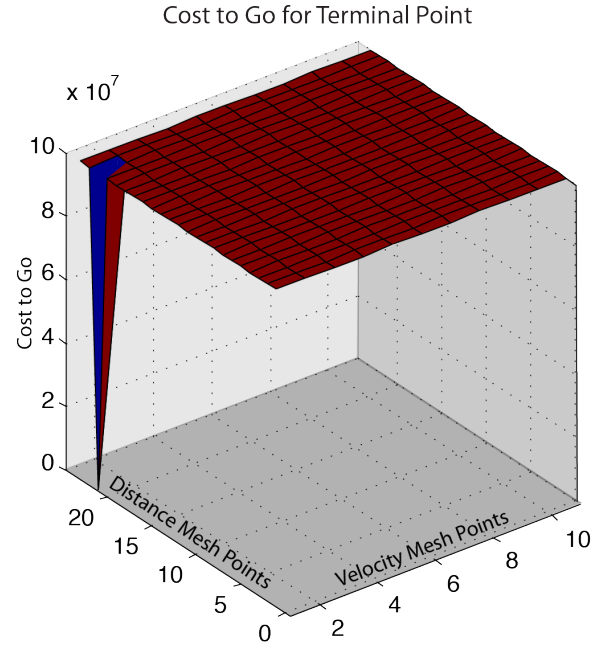


Figure 6: Cost to go matrix set to a zero value at the desired terminal point and an “infinite” value everywhere else.

Finding the transition cost matrix is computationally expensive using FSOLVE. To mitigate this effect we solved equations 7-11 for the coarse state and input meshes and then interpolated between the points on the mesh. MATLAB has a built-in function, INTERPN, which can interpolate on an n-dimensional matrix. We used linear interpolation to increase mesh resolution by a factor of two as seen below in Table 2. This does increase the computational cost of the dynamic program but it is more computationally efficient than actually increasing our mesh resolution for the transition cost matrix. It should be noted that there is some corresponding decrease in accuracy with this linear interpolation although no formal analysis was done in this study.

To calculate the new states on the time mesh we used forward Euler integration as a method of approximation. Without careful planning of mesh size it requires the use of some “reverse interpolation”. We used nearest neighbor

Table 2: State and Input Mesh Refinement

Variable	Coarse Mesh	Fine Mesh
x_1	0 : 5 : 25	0 : 2.5 : 25
x_2	0 : 100 : 1100	0 : 50 : 1100
x_3	1290 : 5 : 1330	1290 : 2.5 : 1330
$u_1(10^3)$	-50: 12.5 : 50	-50 : 6.25 : 50
u_2	-450 : 112.5 : 450	-450 : 56.25 : 450

interpolation to compare each newly calculated state value to the corresponding state mesh. This method forces the state value to the closest mesh point; the dynamic program uses this estimated point to calculate the next step backwards.

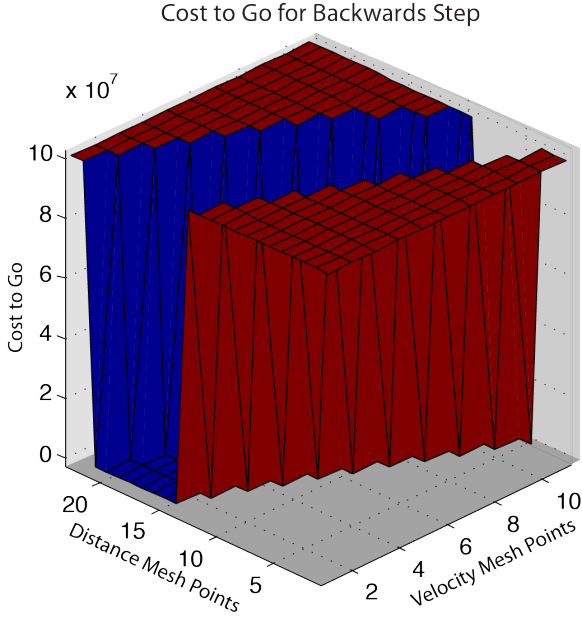


Figure 7: Cost to go matrix for a backwards step showing the potential paths for the velocity to follow.

2.5 Assumptions

In the course of developing our dynamic and static equations several assumptions were made in order to simplify our analysis:

1. The flywheel is in a vacuum and resting on magnetic bearings, which are features in most modern systems. This allows us to neglect friction and windage losses in our mechanical state equations.
2. The flywheel will not mechanically fail at any point within the operating range used in our simulation.
3. The subway car is modeled as a rectangular box, and therefore aerodynamic drag is based on cross sectional

area.

4. Based on values provided within the literature, the following constants were used:

- a. Train car mass: 50,000 *kg*
- b. Flywheel mass: 2,500 *kg*
- c. Flywheel radius: 0.6 *m*
- d. Rolling resistance coefficient: 0.005
- e. Aerodynamic drag coefficient: 0.6
- f. Air density: 1.2 *kg/m³*
- g. Frontal area: 9.29 *m²*
- g. Substation Losses (R'): 0.0013 Ω

5. The track which the subway train follows is perfectly straight and level, containing no grades or misalignment.
6. The track material is isotropic and therefore has a constant resistance of 24.6 *m Ω /km*.
7. The external power supply has an infinite ability to deliver or absorb energy as dictated by the system.
8. Our process is cyclic and assumes subway trains are departing and arriving from stations at a constant, synchronized rate. This means the flywheel will always return to its initial state of charge.

3 Results

Running the DDP simulation produced the plots shown in Figures 8 and 9. The plot of train velocity at each time step in Figure 8 (A) validates our requirements of the train traveling 1000 *m* in 120 seconds without the velocity increasing over 20 *m/s* and ending at the terminal velocity state of 0 *m/s* at the second station.

The plot of flywheel velocity at each time step in Figure 8 (B) validates our requirements of the flywheel returning to the initial velocity value at the end of the run without dropping below 1290 *rad/s*. To confirm that all states converged to their specified terminal value, Figure 9 was included to show that the distance requirements were also satisfied in the pre-determined time frame.

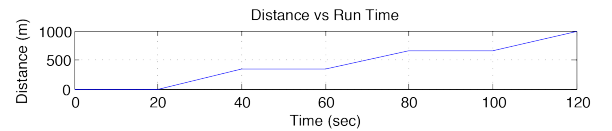


Figure 9: Distance the train has travelled at each time step.

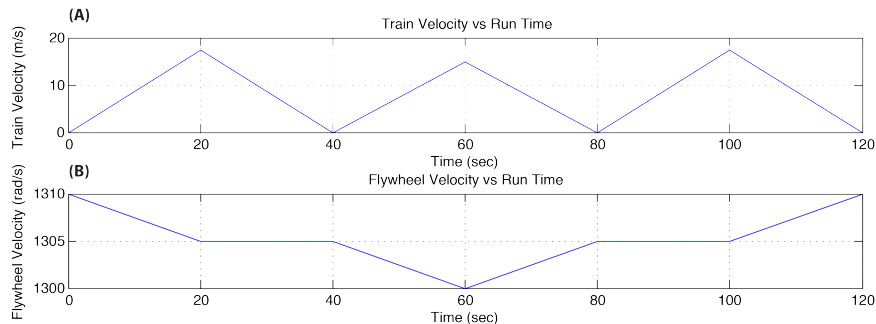


Figure 8: Plots obtained from the DDP simulation. (A) Train velocity at each time step, (B) Flywheel velocity at each time step.

Comparing the velocity profile of the train to the velocity profile of the flywheel shows that the flywheel decreases in speed as the train accelerates during the first time step and holds steady as the train brakes during the second time step. The energy from the train is sold back to the power supply rather than being stored in the flywheel during this regenerative braking period. During the second train acceleration the flywheel is being drained to supplement what is being drawn from the power supply. As the train decelerates a second time, the distance it has traveled nears the halfway point where the flywheel is positioned, therefore the flywheel absorbs some of the energy because rail losses would be the lowest along the trip. The final train acceleration does not affect the flywheel speed because the flywheel is being forced to return to its initial velocity value, which is validated as the final train deceleration returns the flywheel to its required terminal velocity value; the rest of the energy is sold back to the power supply.

4 Conclusions

In the final analysis we determined that our results were accurate within the constraints of the problem along with the many assumptions that we made, however they are not viable in a realistic context. The biggest drawback of our simplifications was the “efficiency” being calculated as a resistive loss. This was a problem because our method did not accurately capture the effect of a real motor efficiency map, which would have lower efficiencies at low speeds and high torques, and higher efficiencies at high speeds and moderate torques. Our approach with resistive losses resulted in very high efficiency values at lower speeds and power losses that increased quadratically as current increased. This shows an inverse relationship from what the efficiencies should have been compared to what are simulation produced.

The flywheel velocity changed appropriately given the static algebraic constraints that were applied and the train velocity profile which was produced. This shows that our

relationship between train and flywheel velocity was accurate. Overall, the DDP algorithm converged to the terminal state values that we specified in the time frame required. This implies that the transition cost matrix that was pre-calculated was implemented correctly into the simulation and preserves the cyclic requirement of the system. We also ran a case where the flywheel was forced to stay at the same speed and not absorb or disperse energy to the train, and since the train velocity profile didn’t change we can say that there is a potential for cost savings with the flywheel storage system.

5 Future Work

Given enough time and computing power we would make our state meshes much finer, resulting in increasingly accurate results. Also, this accuracy could be enhanced by performing a comparative study of the interpolation parameters used to add detail to the transition cost matrix. Therefore, appropriate efficiency maps should be created and included in the overall model.

Additional candidates for reevaluation are our various mechanical characteristics; the train car weight, size, and passenger capacity as well as the flywheel energy capacity, speed, and size. Along the same lines, the track model itself could be improved, incorporating the various grades and curves which are inherent in many systems.

An even more fundamental obstacle to consider is the assumed cyclic nature of the mass transit system, which is currently relatively simple. Given the chance, we could implement some aspects of an imperfect case, such as to varying station distances, train frequencies, and station capacities; this problem may be better modeling with stochastic dynamic programming (SDP) rather than DDP. Lastly, our overall structure of a single flywheel/two station design could be altered to the more ideal two flywheel/two station design which was previously disregarded due to dimensional complexity and the associated time and computing costs.

6 Acknowledgements

The authors would like to express their deep appreciation for Dr. Hosam Fathy of The Pennsylvania State University to his guidance, support, and enthusiasm. Additionally, his Fall 2011 course “Optimal Control of Energy Systems” provided much of the foundation for concepts developed in this project.

A Case 2 Constraint Equations

The second case of algebraic constraints for when the train passes the midpoint of the run are as follows:

$$I_1 = I_3 + I_4 \quad (12)$$

$$I_3 = I_2 + I_5 \quad (13)$$

$$\begin{aligned} u_1 x_1 = & I_2(V_0 - I_1(R' + \frac{R}{D}(0.5D))) \\ & - I_3 \frac{R}{D}(x_2 - 0.5D) - I_2 R_{MG} \end{aligned} \quad (14)$$

$$u_2 x_3 = I_4(V_0 - I_1(R' + \frac{R}{D}(0.5D))) - I_4 R_{FW} \quad (15)$$

$$\begin{aligned} -I_1(R' + \frac{R}{D}(0.5D)) = \\ I_5(R' + \frac{R}{D}(D - x_2)) + I_3 \frac{R}{D}(x_2 - 0.5D) \end{aligned} \quad (16)$$

References

- [1] Bae, Chang Han. “A Simulation Study of Installation Locations and Capacity of Regenerative Absorption Inverters in DC 1500V Electric Railways System.” *Simulation Modeling Practice and Theory* **17.5** (2009): 829–38. Print.
- [2] Rohde, Mike. “Metrobits.org - Metro, Subway, MRT, U-Bahn, Metrorail.” Metrobits. Web. 15 Dec. 2011. <http://mic-ro.com/metro/>.
- [3] Lawson, L. J. “The Kinetic Energy Wheel: A Means of Reducing Pollution While Conserving Resources.” *Institute of Environmental Sciences* **1.21** (1975): 130–33. Print.
- [4] Tester, J. W. “Energy Transfer, Conversion and Storage.” E-Resource. MIT. Web. 15 Dec. 2011. <http://eresourcecenter.org/kc/CourseWare/MitSustainable/Conversion>.
- [5] Hebner, Robert, Joseph Beno, and Alan Walls. “Flywheel Batteries Come Around Again.” *IEEE Spectrum* Apr. 2002: 46–51. Print.
- [6] “Flywheels: Energy-Saving Way to Go.” *Environmental Science & Technology* **10.7** (1976): 636–39. Print.
- [7] “MTA Flywheels Save a Lot of Energy.” *Railway Age* **178.1** (1977). Print.
- [8] Viswanathan, C. N., R. W. Longman, and G. A. Domoto. “Energy Conservation in Subway Systems by Controlled Acceleration and Deceleration.” *Energy Resource* **2** (1978): 133–51. Print.
- [9] Flanagan, R. C., and L. A. Suokas. “Regenerative Drive for Subway Trains—Part 1: Mechanical Accumulator Design.” *Journal of Engineering for Industry* **98.3** (1976): 737. Print.
- [10] Suokas, L. A., and R. C. Flanagan. “Regenerative Drive for Subway Trains—Part 2: Overall System Model.” *Journal of Engineering for Industry* **98.3** (1976): 744. Print.
- [11] Flanagan, R. C., and L. A. Suokas. “Regenerative Drive for Subway Trains—Part 3: System Evaluation.” *Journal of Engineering for Industry* **98.3** (1976): 751. Print.
- [12] Suokas, L. A., and R. C. Flanagan. “Regenerative Drive for Subway Trains—Part 4: Overall System Performance.” *Journal of Engineering for Industry* **98.3** (1976): 756. Print.
- [13] Lawson, L. J., John Koper, and Leonard Cook. “Way-side Energy Storage for Recuperation of Potential Energy from Freight Trains.” *IECEC Conference* **1** (1981): 875–80. Print.
- [14] Lawson, L. J. “Application of Kinetic Energy Storage to Transportation Systems.” *High Speed Ground Transportation Journal* **12.3** (1978): 1–27. Print.
- [15] Barrero, R., X. Tackoen, and J. Van Mierlo. “Stationary or Onboard Energy Storage Systems for Energy Consumption Reduction in a Metro Network.” *Proceedings of the Institution of Mechanical Engineers, Part F: Journal of Rail and Rapid Transit* **224.3** (2010): 207–25. Print.
- [16] Radcliffe, P., J. S. Wallace, and L. H. Shu. “Stationary Applications of Energy Storage Technologies for Transit Systems.” *IEEE Electrical Power & Energy Conference* (2010): 1–7. Print.
- [17] Bertsekas, D. P. *Dynamic Programming and Optimal Control*. Belmont, MA: Athena Scientific, 1995. Print.